High slope efficiency and high refractive index change in direct-written Yb-doped waveguide lasers with depressed claddings

Guido Palmer,[1,2,*] Simon Gross,[1] Alexander Fuerbach,[1] David G. Lancaster,[3] and Michael J. Withford[1]

[1]*Centre for Ultrahigh bandwidth Devices for Optical Systems (CUDOS), MQ Photonics Research Centre, Department of Physics and Astronomy, Macquarie University, North Ryde, New South Wales 2109, Australia*
[2]*European XFEL GmbH, Albert-Einstein-Ring 19, 22761 Hamburg, Germany*
[3]*Institute for Photonics and Advanced Sensing, School of Chemistry & Physics, University of Adelaide, Adelaide, South Australia, 5005, Australia*
[*]*guido.palmer@xfel.eu*

Abstract: We report the first Yb:ZBLAN and Yb:IOG10 waveguide lasers fabricated by the fs-laser direct-writing technique. Pulses from a Titanium-Sapphire laser oscillator with 5.1 MHz repetition rate were utilized to generate negative refractive index modifications in both glasses. Multiple modifications were aligned in a depressed cladding geometry to create a waveguide. For Yb:ZBLAN we demonstrate high laser slope efficiency of 84% with a maximum output power of 170 mW. By using Yb:IOG10 a laser performance of 25% slope efficiency and 72 mW output power was achieved and we measured a remarkably high refractive index change exceeding $\Delta n = 2.3 \times 10^{-2}$.

OCIS codes: (140.3615) Lasers and laser optics; (130.2755) Integrated optics.

References and links

1. S. Nolte, M. Will, J. Burghoff, and A. Tünnermann, "Femtosecond waveguide writing: a new avenue to three-dimensional integrated optics," App. Phys. A **77**, 109–111 (2003) http://link.springer.com/article/10.1007/s00339-003-2088-6
2. R. Osellame, H. J. W. M. Hoekstra, G. Cerullo, and M. Pollnau, "Femtosecond laser microstructuring: an enabling tool for optofluidic lab-on-chips," Laser Photon. Rev. **5**(3), 442–463 (2011), doi:10.1002/lpor.201000031.
3. A. Crespi, R. Ramponi, R. Osellame, L. Sansoni, I. Bongioanni, F. Sciarrino, G. Vallone, and P. Mataloni, "Integrated photonic quantum gates for polarization qubits," Nat. Commun. **2**, (2011) http://www.nature.com/ncomms/journal/v2/n11/full/ncomms1570.html
4. C. Grivas, "Optically pumped planar waveguide lasers, Part I: Fundamentals and fabrication techniques," Prog. Quant. Electron. **35**, 159–239 (2011) http://www.sciencedirect.com/science/article/pii/S0079672711000139
5. M. Ams, P. Dekker, G. D. Marshall, and M. J. Withford, "Monolithic 100 mW Yb waveguide laser fabricated using the femtosecond-laser direct-write technique," Opt. Lett. **34**(3), 247–249 (2009), http://www.opticsinfobase.org/ol/abstract.cfm?URI=ol-34-3-247.
6. E. H. Bernhardi, H. A. G. M. van Wolferen, K. Wörhoff, R. M. de Ridder, and M. Pollnau, "Highly efficient, low-threshold monolithic distributed-Bragg-reflector channel waveguide laser in Al_2O_3:Yb^{3+}," Opt. Lett. **36**(5), 603–605 (2011), http://www.opticsinfobase.org/ol/abstract.cfm?URI=ol-36-5-603.
7. A. Choudhary, A. A. Lagatsky, P. Kannan, W. Sibbett, C. T. A. Brown, and D. P. Shepherd, "Diode-pumped femtosecond solid-state waveguide laser with a 4.9 GHz pulse repetition rate," Opt. Lett. **37**(21), 4416–4418 (2012), http://www.opticsinfobase.org/ol/abstract.cfm?URI=ol-37-21-4416.
8. D. G. Lancaster, S. Gross, H. Ebendorff-Heidepriem, K. Kuan, T. M. Monro, M. Ams, A. Fuerbach, and M. J. Withford, "Fifty percent internal slope efficiency femtosecond direct-written Tm^{3+}:ZBLAN waveguide laser," Opt. Lett. **36**(9), 1587–1589 (2011), http://www.opticsinfobase.org/ol/abstract.cfm?URI=ol-36-9-1587.
9. S. Taccheo, G. D. Valle, R. Osellame, G. Cerullo, N. Chiodo, P. Laporta, O. Svelto, A. Killi, U. Morgner, M. Lederer, and D. Kopf, "Er:Yb-doped waveguide laser fabricated by femtosecond laser pulses," Opt. Lett. **29**(22), 2626–2628 (2004), http://www.opticsinfobase.org/ol/abstract.cfm?URI=ol-29-22-2626.

10. S. Müller, T. Calmano, P. Metz, N.-O. Hansen, C. Kränkel, and G. Huber, "Femtosecond-laser-written diode-pumped Pr:LiYF$_4$ waveguide laser," Opt. Lett. **37**(24), 5223–5225 (2012), http://www.opticsinfobase.org/ol/abstract.cfm?URI=ol-37-24-5223.
11. C. Grivas, C. Corbari, G. Brambilla, and P. G. Lagoudakis, "Tunable, continuous-wave Ti:sapphire channel waveguide lasers written by femtosecond and picosecond laser pulses," Opt. Lett. **37**(22), 4630–4632 (2012), http://www.opticsinfobase.org/ol/abstract.cfm?URI=ol-37-22-4630.
12. T. Calmano, J. Siebenmorgen, A.-G. Paschke, C. Fiebig, K. Paschke, G. Erbert, K. Petermann, and G. Huber, "Diode pumped high power operation of a femtosecond laser inscribed Yb:YAG waveguide laser," Opt. Mater. Express **1**(3), 428–433 (2011), http://www.opticsinfobase.org/aop/fulltext.cfm?uri=ome-1-3-428&id=219315.
13. R. Mary, S. J. Beecher, G. Brown, R. R. Thomson, D. Jaque, S. Ohara, and A. K. Kar, "Compact, highly efficient ytterbium doped bismuthate glass waveguide laser," Opt. Lett. **37**(10), 1691–1693 (2012), http://www.opticsinfobase.org/ol/abstract.cfm?URI=ol-37-10-1691.
14. M. Ams, G. D. Marshall, P. Dekker, J. A. Piper, and M. J. Withford, "Ultrafast laser written active devices," Laser Photonics Rev. **3**, 535–544 (2009) http://onlinelibrary.wiley.com/doi/10.1002/lpor.200810050/abstract
15. S. Gross, M. Ams, D. G. Lancaster, T. M. Monro, A. Fuerbach, and M. J. Withford, "Femtosecond direct-write überstructure waveguide Bragg gratings in ZBLAN," Opt. Lett. **37**(19), 3999–4001 (2012), http://www.opticsinfobase.org/ol/abstract.cfm?URI=ol-37-19-3999.
16. P. Dekker, M. Ams, G. D. Marshall, D. J. Little, and M. J. Withford, "Annealing dynamics of waveguide Bragg gratings: evidence of femtosecond laser induced colour centres," Opt. Express **18**(4), 3274–3283 (2010), http://www.opticsinfobase.org/oe/abstract.cfm?URI=oe-18-4-3274.
17. S. M. Eaton, H. Zhang, M. L. Ng, J. Li, W.-J. Chen, S. Ho, and P. R. Herman, "Transition from thermal diffusion to heat accumulation in high repetition rate femtosecond laser writing of buried optical waveguides," Opt. Express **16**(13), 9443–9458 (2008), http://www.opticsinfobase.org/oe/fulltext.cfm?uri=oe-16-13-9443&id=163577.
18. S. Gross, M. Ams, G. Palmer, C. T. Miese, R. J. Williams, G. D. Marshall, A. Fuerbach, D. G. Lancaster, H. Ebendorff-Heidepriem, and M. J. Withford, "Ultrafast Laser Inscription in Soft Glasses: A Comparative Study of Athermal and Thermal Processing Regimes for Guided Wave Optics," Int. J. Appl. Glass Sci. **3**(4), 332–348 (2012), doi:10.1111/ijag.12005 (IJAGS).
19. A. M. Streltsov and N. F. Borrelli, "Study of femtosecond-laser-written waveguides in glasses," J. Opt. Soc. Am. B **19**(10), 2496 (2002), http://www.opticsinfobase.org/josab/abstract.cfm?uri=josab-19-10-2496.
20. B. M. Walsh and N. P. Barnes, "Comparison of Tm:ZBLAN and Tm:silica fiber lasers; Spectroscopy and tunable pulsed laser operation around 1.9 µm," App. Phys. B **78**, 325–333 (2004) http://link.springer.com/article/10.1007%2Fs00340-003-1393-2?LI=true#
21. D. G. Lancaster, S. Gross, A. Fuerbach, H. E. Heidepriem, T. M. Monro, and M. J. Withford, "Versatile large-mode-area femtosecond laser-written Tm:ZBLAN glass chip lasers," Opt. Express **20**(25), 27503–27509 (2012), http://www.opticsinfobase.org/oe/abstract.cfm?uri=oe-20-25-27503.
22. R. Osellame, N. Chiodo, V. Maselli, A. Yin, M. Zavelani-Rossi, G. Cerullo, P. Laporta, L. Aiello, S. De Nicola, P. Ferraro, A. Finizio, and G. Pierattini, "Optical properties of waveguides written by a 26 MHz stretched cavity Ti:sapphire femtosecond oscillator," Opt. Express **13**(2), 612–620 (2005), http://www.opticsinfobase.org/oe/abstract.cfm?URI=oe-13-2-612.
23. D. Findlay and R. A. Clay, "The measurement of internal losses in a 4-level-lasers," Phys. Lett. **20**(3), 277–278 (1966), http://www.sciencedirect.com/science/article/pii/0031916366903635.
24. S. Gross, D. G. Lancaster, H. Ebendorff-Heidepriem, T. M. Monro, A. Fuerbach, and M. J. Withford, "Femtosecond laser induced structural changes in fluorozirconate glass," Opt. Mater. Express **3**(5), 574–583 (2013), http://www.opticsinfobase.org/ome/abstract.cfm?URI=ome-3-5-574.

1. Introduction

Integrated photonic devices are gaining in scientific and industrial importance since they offer complex circuitry and hybrid functionality on a small footprint [1–3]. Moreover, their monolithic nature results in an inherent robustness and low noise operation. Waveguide lasers (WGLs) are ideal radiation sources for such photonic networks due to their small footprint, high efficiency and excellent beam quality which permit on-chip integration and low loss single-mode coupling [4]. In addition to CW-operation with narrow linewidth [5,6], in recent times femtosecond mode-locked WGL have attracted particular interest as they offer tens-of-GHz repetition rates [7].

WGLs have been demonstrated in various rare-earth doped glasses and crystals that cover a broad spectral range [8–11]. In particular, Ytterbium-doped media emitting around 1 micron offer high absorption and emission cross-sections along with a low quantum defect that makes them ideal for high-power direct diode-pumping with a low thermal load. For direct laser written devices Yb-WGLs hold the current records regarding output power (2.35 W [12],) and slope efficiency (79% [13],), respectively.

The direct laser writing technique is a well established method for the fabrication of WGL in dielectric materials [14]. In contrast to other fabrication methods, it offers the advantage of a rapid single-step fabrication with the potential for inscription of 3D photonic architectures [1]. Additionally, Bragg-gratings can be directly incorporated during the same processing step to create a monolithic laser with narrow linewidth output [5,15].

The long-term stability of direct laser-written WGLs (especially in glasses) strongly depends on the host material, the fabrication parameters and the type of induced structural modifications within the host material. Previously, direct-written Yb-doped phosphate glass WGLs suffered from self-annealing during operation that leads to degradation of the waveguides and the incorporated Bragg-gratings [16]. These WGLs were written in the athermal regime with kHz-repetition rate femtosecond pulses that gave rise to a positive refractive index change (RIC). In contrast, writing with higher repetition rates result in cumulative heating [17] which yields a negative RIC in a large number of glasses [18]. However, MHz laser written structures exhibit high temperature stabilities [18,19] which makes them attractive for the fabrication of highly robust WGLs.

Even though the femtosecond laser may induce a negative RIC, waveguides can still be created by arranging modifications around an unmodified volume to create a depressed cladding (DC) [15]. In this investigation we concentrated on finding and evaluating suitable Yb-doped glasses that provide long-run RIC stability for WGL operation.

Fluorozirconate glasses, in particular ZBLAN, have attracted a great deal of attention for fiber laser applications beyond 1 µm wavelength, where some of its material properties are superior to silica glasses [20]. Previous experiments have shown that ZBLAN is an excellent candidate for short-IR WGLs emitting around 2 µm fabricated by MHz repetition rate femtosecond pulses [8, 21]. The advantages of ZBLAN include an outstanding WG circularity and an excellent reproducibility of the laser written modifications. In this paper we evaluate Yb doped ZBLAN glass and compare its performance with other Yb doped glasses. While it became clear that Yb:IOG1, a commercial phosphate glass from Schott, is not suited for our purposes [18], Yb:IOG10, a silicate glass (Schott), was a more encouraging candidate based on previous studies [22]. In the latter a MHz-laser was utilized to fabricate reasonably circular modifications with negative RIC in undoped IOG10. For each material we discuss specific fabrication requirements, waveguide properties and lasing performance.

2. Waveguide laser fabrication and guiding properties

Before commencing the writing process, chip-sized samples were prepared by dicing, grinding and polishing to optical quality. After laser inscription the end-facets were ground and polished to reveal the waveguide ends. The final 2.5 mol% ytterbium doped ZBLAN WGL-sample was 9 mm long with small regions outside the WG structure containing crystals. Higher doping concentrations could not be tested due to crystallization reducing glass yield during production. The Yb:IOG10 sample was prepared in the same manner to obtain a 10 mm long laser chip with a dopant concentration of 8.0 wt%.

The fabrication laser delivers 45 fs short pulses at a repetition rate of 5.1 MHz and maximum pulse energies of 550 nJ (Femtolasers, Femtosource XL). A set of air-bearing translation stages (Aerotech) was used to translate the samples while the laser beam was focused by either a 1.25 NA (Zeiss N-Achroplan) or 1.4 NA (Olympus SPlan-APO) oil immersion objective (both 100 × magnification). Only circular polarized pulses were utilized.

In the case of Yb:ZBLAN we used the 1.25 NA microscope objective with a physical working distance of 450 µm and the sample was translated at a speed of 1000 mm/min. From our experiences with other rare-earth doped ZBLAN lasers these parameters produce a circular symmetric waveguide [Fig. 1(a)] with a high reproducibility of the modified regions [8,10].

With the given repetition rate and pulse energies around 80 nJ, the typical negative RIC is in the range of $\Delta n \approx -1.2 \times 10^{-3}$ for a single pass writing process [18]. The resulting

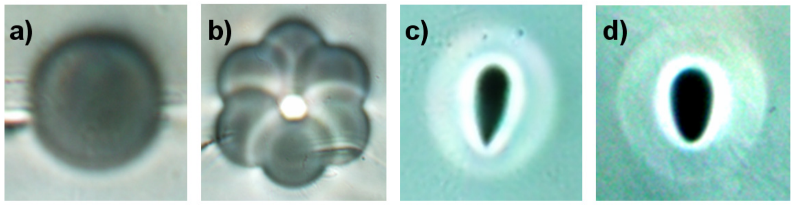

Fig. 1. Cross-sectional microscope images (laser incident from the top) of: (a) single modification in Yb:ZBLAN (80 nJ, 1000 mm/min), (b) depressed cladding in Yb:ZBLAN (identical fabrication parameters), (c) single modification in Yb:IOG10 (1.25 NA objective), (d) Yb:IOG10: reduced pointiness of the bottom tip by utilizing the 1.4 NA objective; (arbitrary magnifications).

modification diameter is approximately 32 µm [Figs. 1(a)–1(b)]. A total of 6 modifications were arranged in a ring geometry to form a depressed cladding in the Yb:ZBLAN sample at a center depth of 300 µm. Waveguides with core diameters ranging from 5 - 15 µm were inscribed by changing the diameter of the ring while keeping all other parameters constant. Figure 1(b) shows an image of an optimized WGL with a core diameter of 13 µm.

We probed waveguides for their mode-field profiles at the wavelength of λ_{pump} = 974 nm and λ_{laser} = 1030 nm by imaging the near-field intensity distribution onto a CCD-camera. Single mode-guiding was found for all core diameters from 6 µm to 14 µm (multimode for larger diameters). However waveguides with core diameters below 11 µm suffered from stress-fractures across their cores. For core sizes between 10 – 14 µm the mode-field diameters (MFD) changed from 12 to 14 µm (4σ-values). Figure 4(a) illustrates the mode-field profile of the 13 µm core diameter WG used for the laser experiments.

As mentioned previously, Yb:phosphate WGLs suffer from self-annealing when being pumped at 974 nm (strongest alteration within first 30 min [16].). To investigate the stability of Yb:ZBLAN and Yb:IOG10 waveguides, their mode-field profile was monitored over a period of 24 hours while being pumped by > 400 mW of 974 nm laser radiation. However for Yb:ZBLAN and Yb:IOG10 no change of MFD could be observed [Fig. 2(a)].

In the case of Yb:IOG10 a different modification morphology was revealed compared to Yb:ZBLAN when using identical writing parameters. Hence a comprehensive and iterative study on writing parameters for Yb:IOG10 was carried out and modifications were arranged in different geometries to evaluate their applicability for WGL operation.

As depicted in Figs. 1(c) and 1(d) single modifications consist of a wide outer region of positive RIC (bright regions) surrounding a thin band of stronger positive RIC. The latter encloses a large volume with negative RIC (dark centre). By using the 1.25 NA oil immersion objective, the modification cross-sections resemble a tear-drop-like shape with a tip pointing downwards in the direction of the fs-laser propagation. This makes it difficult to align multiple modifications in order to form a depressed cladding with a homogeneous shape.

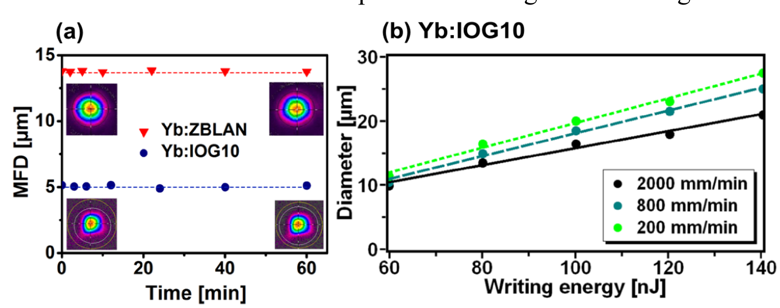

Fig. 2. (a) MFD as function of pump duration (insets: start profiles [left] and profiles after 24 hrs pumping [right]). (b) Average modification size (vert. and horiz. data points) versus writing speed and pulse energy for Yb:IOG10.

#191288 - $15.00 USD Received 28 May 2013; revised 30 Jun 2013; accepted 1 Jul 2013; published 12 Jul 2013

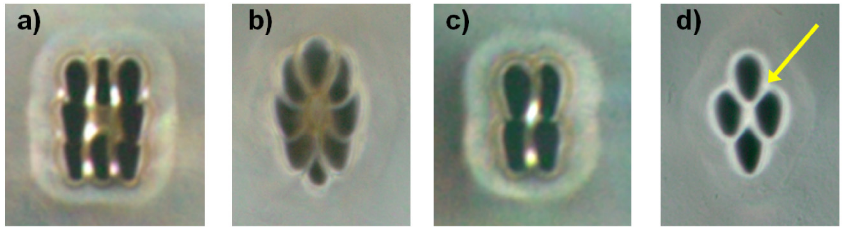

Fig. 3. Selection of investigated waveguide geometries in Yb:IOG10. The writing laser beam was incident from the top. The arrow highlights the principle location of additional waveguide structures.

Thus our goal was to reduce the asymmetry and reach the best possible circular shape. Efficient suppression of the tip was achieved by utilizing the 1.4 NA microscope objective because of the larger cone angle of the focused light resulting from the objective's higher numerical aperture. Additionally, lower writing speeds (below 100 mm/min) helped to improve the circular symmetry. Remarkably, any writing speed from 10 – 2000 mm/min provided straight and homogenous modifications along the translation direction without damage or void formation. Higher pulse energies led to an increase of modification volume and magnitude of the RIC. Figure 2(b) illustrates the dependence of modification size on laser writing speed and pulse energy. Optical damage occurred for pulse energies exceeding 140 nJ. As a consequence of the short working distance for the objective the operation depth was limited to values between 120 – 180 µm. Outside these thresholds structural irregularities and damage occurred.

Through the study we found that combining a pulse energy of 90 nJ with a writing speed of 20 mm/min gave the most appropriate modifications for depressed claddings [Fig. 3]. However, the resulting modifications are still elliptical and retain a slight asymmetry.

Because the modifications in Yb:IOG10 are not as circular symmetric than in ZBLAN various different modification arrangements were evaluated to obtain a low loss single-mode waveguide [Fig. 3]. Different RIC regions can be identified depending on the number N of modifications superimposed to form a waveguide.

For N > 4 we observed a degradation of the glass transmission mainly where the intended WG-cores are located (brownish appearing areas in Figs. 3(a)-3(b)). For N ≤ 4 and for intermediate regions of N > 4 waveguides were formed (bright white areas) between depressed regions [Figs. 3(a), 3(c)-3(d)]. Furthermore, lossy waveguiding was also observed in areas highlighted by the arrow in Fig. 3(d). Typical WG core sizes are between 4 and 8 µm. The distances between modifications had to be thoroughly chosen to obtain effective circular guiding regions. Of all the investigated geometries, the waveguides depicted in Fig. 3(c) were superior with regard to transmission efficiency, beam circularity, single-mode guiding and laser performance. Two main waveguides can be identified in the modification volume. The first WG is situated in the center of the structure, whereas a second WG is present beneath the center WG.

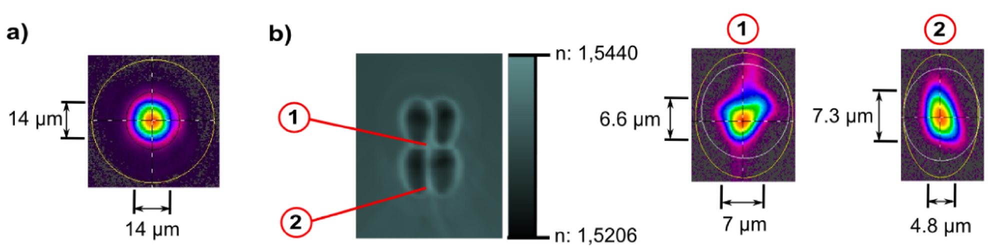

Fig. 4. Mode field profiles at λ = 974 nm: (a) Yb:ZBLAN-WG, (b) Yb:IOG10: measured refractive index profile (left) of the structure in Fig. 3(c) and mode-field profiles (right) of the waveguides at location 1 and 2.

The mode of the center waveguide shown in Fig. 4(b) features extended wings along the thin positive refractive index boundaries between modifications [i.e. Figure 4(b1)].
The waveguide's single-modedness was tested via transverse translation of the injection optics to excite higher-order modes. However, no change in the mode shape was observed.

Figure 4(b) shows the refractive index profile and mode-field profiles at 974 nm of the waveguide geometry in Fig. 3(c). The refractive index profile of the Yb:IOG10-WG was measured with a refracted near-field profilometer (RINCK Elektronik). The refractive index change was taken as the difference in the RI value from the center of the waveguide (bright) to the minimum value of the negative index region (dark). We measured peak refractive index differences of $\Delta n = 2.19 \times 10^{-2}$ for the center WG [Fig. 4(b1)] and $\Delta n = 2.34 \times 10^{-2}$ for the lower WG structure [Fig. 4(b2)]. Finally MFDs were measured as function of pump duration for a similar WG with slightly smaller MFD to confirm the absence of self-annealing effects [Fig. 2(a)].

3. Waveguide laser characterization

The Yb:IOG10 and Yb:ZBLAN WGLs were characterized using the setup shown in Fig. 5. Pump radiation was provided by a wavelength stabilized, fiber-coupled 974 nm single mode diode laser.

Launching the diode radiation through a polarization maintaining fiber and subsequent aspheric pump lenses yielded maximum pump powers of 410 mW (Yb:ZBLAN) and 428 mW (Yb:IOG10). The different pump powers result from the different focusing lenses used. A dichroic mirror extracted the backward propagating WGL leakage at 1030 nm from the pump beam path (power < 1mW). A second dichroic mirror was placed at the laser output to separate residual pump from the actual laser radiation. Plan-parallel resonator mirrors were butt-coupled to the WGL-sample with a remaining µm-range air gap between the mirror and the WG. The available output coupler mirrors (OC) provided transmission values at 1030 nm of: 9.5%, 14.7%, 21.5%, 35%. Different WGs were investigated with respect to output power, spectrum, mode-field profile and polarization. The pump optics and the OC-mirror was mounted on piezo-driven translation stages which enabled fine adjustment across 6-axis (x, y, z, θ_x, θ_y, θ_z). The sample itself was placed on a xyz-translation stage.

Since the MFDs were different for both media different focusing lenses were utilized and coupling losses were measured individually. The coupling losses were determined by measuring the focal spot size and the waveguide mode-field profile followed by numerically evaluating the mode-overlap integral based on the recorded images. By including the Fresnel losses we calculated coupling losses of $CL_1 = 2.52$ dB for Yb:ZBLAN and $CL_2 = 0.95$ dB in the case of Yb:IOG10.

The propagation losses (PL) for each material were determined by a Findlay-Clay analysis [23]. For a conservative calculation we estimated the absorbed pump power to be equal to the coupled pump power without including any further losses. This approximation is based on the high reflectivity of the OC-mirrors at the pump wavelength of 974 nm and the calculated absorption in both media.

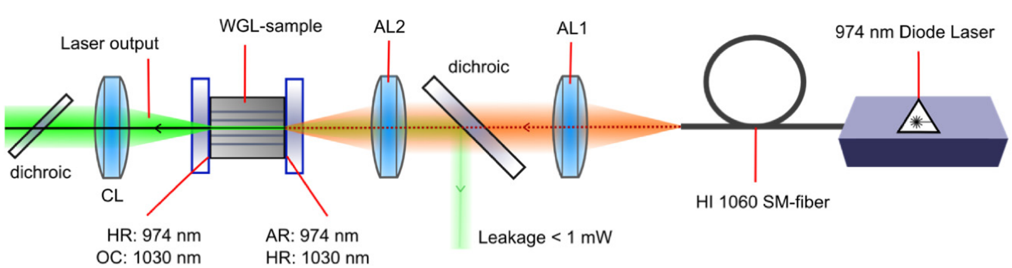

Fig. 5. Schematic of WGL setup, AL: aspheric lens, CL: collimation lens, OC: output coupler.

#191288 - $15.00 USD Received 28 May 2013; revised 30 Jun 2013; accepted 1 Jul 2013; published 12 Jul 2013

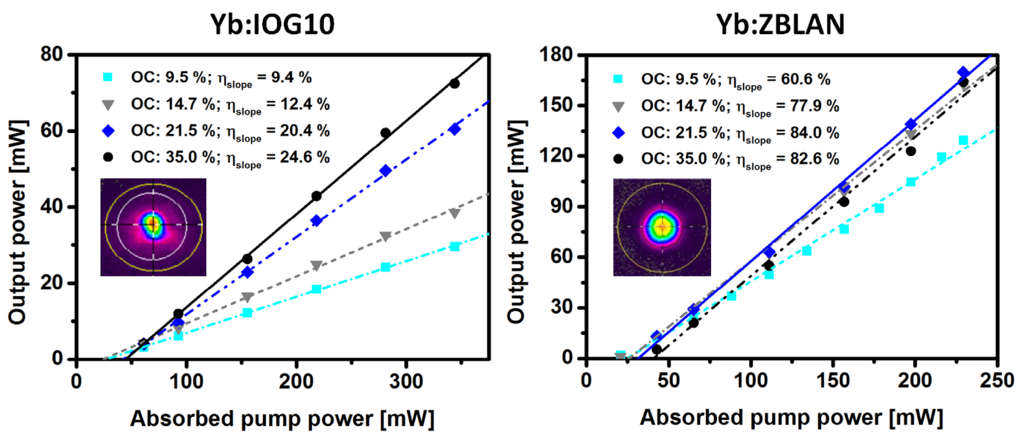

Fig. 6. Output power curves for Yb:IOG10 (left) and Yb:ZBLAN (right) with different OC-mirrors, inset showing far field mode of each guide at maximum output power.

The waveguide shown in Fig. 4(b2) provided the best laser performance in the case of Yb:IOG10. The highest output power of 72 mW was measured with an OC-ratio of almost 35% [Fig. 6]. The lasing threshold was reached at 44 mW absorbed pump power. The related slope efficiency equals η = 24.6% with a total efficiency of 17.5% at maximum pump power (428 mW). The lowest pump power threshold of 26 mW was observed with 9.5% OC-ratio. The Findlay-Clay analysis yielded an upper limit for the propagation loss of PL = 3.45 dB/cm. For all investigated Yb:IOG10-WGLs we determined an average PL-value of 3 dB/cm. An optical spectrum analyzer with a resolution of 10 pm was utilized to measure the output wavelength. The spectrum in Fig. 7 was taken at maximum output power with the 35% OC. Single resonator modes are identifiable in the modulated envelope of the spectrum. The polarization ratio of the laser output increased with higher powers to a maximum value of 10:1.

The Yb:ZBLAN-WGLs were characterized in the same fashion. A maximum output power of 170 mW was reached with 21.5% output coupling [Fig. 6]. Taking the estimated absorbed pump power into account the slope efficiency exceeded 80% for both the 21.5% and 35% OC-mirror. At the maximum output power the total efficiency equals 41% with respect to the incident pump power.

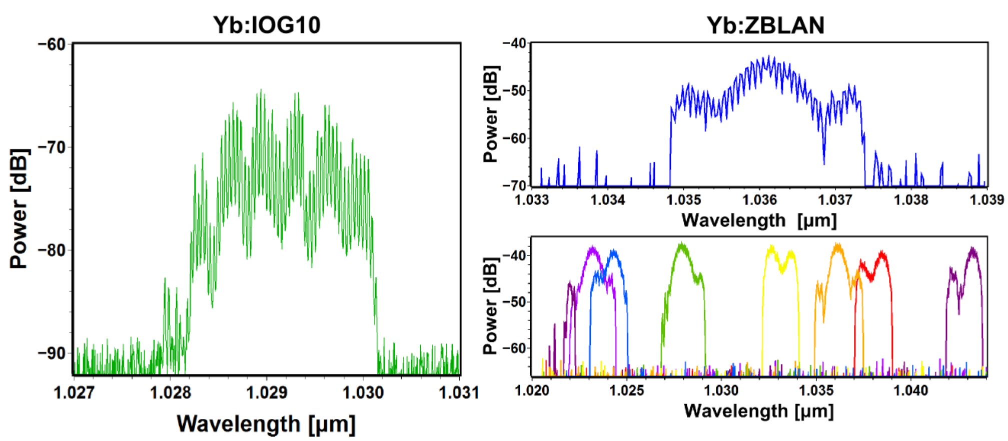

Fig. 7. Yb:IOG10 power spectrum (left) measured at maximum output power (Δλ = 0.01 nm); Yb:ZBLAN spectra (right): top showing high resolved spectrum Δλ = 0.01 nm at 1036 nm centre wavelength and lower illustrates free running wavelength loop observed within approximately 12 min.

#191288 - $15.00 USD Received 28 May 2013; revised 30 Jun 2013; accepted 1 Jul 2013; published 12 Jul 2013

The lasing threshold for the 21.5% OC-configuration was found at 31 mW whereas the lowest threshold power of 25 mW was observed with the lowest OC-ratio (9.5%). Based on the Findlay-Clay analysis a propagation loss of PL = 0.7 dB/cm was found. This propagation loss is substantially lower than the Yb:IOG10 value which explains the significantly better performance of Yb:ZBLAN. While the spectrum of Yb:IOG10 was relatively stable during operation, the Yb:ZBLAN spectrum was occasionally drifting in a loop between 1020 and 1045 nm over a period of 12 minutes without any significant change in output power. Once the gain at the opposite end of the spectral drift range became higher the laser's center wavelength jumped from 1045 nm back down to 1020 nm and started drifting towards 1045 nm again. We attribute this behavior to thermal drifts in the experimental setup that continuously changed the etalon formed by the air gap between OC and WG. Occasionally a sinusoidal variation in the output power ($\Delta P \approx 30\%$) of the Yb:ZBLAN WGL occurred that originated from a rotation of output polarization state. The full-cycle period was in the range of half a minute and was observed as constant power change behind both outputs of a polarizer.

6. Conclusion

In summary we utilized a high repetition rate fs-laser to fabricate waveguide lasers in Yb:IOG10 and Yb:ZBLAN glass based on depressed cladding waveguides. For both media we determined fabrication parameters and characterized the WG properties to confirm that they are long-term stable under laser operation. Furthermore, we measured a high RIC of up to $\Delta n = 2.3 \times 10^{-2}$ in Yb:IOG10. The waveguide propagation losses of Yb:IOG10 were more than 2 dB/cm higher than that of Yb:ZBLAN which resulted in a substantially lower laser slope efficiency of 25%. We observed superior slope efficiencies in Yb:ZBLAN in excess of 80% with up to 170 mW output power. With an optimized pump focusing lens it should be possible to greatly improve the coupling efficiency and therefore the maximum output power in forthcoming experiments. While in Yb:ZBLAN perfect circular modifications could be created, the Yb:IOG10 silica glass yields more complex RI-modifications with a greater non-uniformity. To reduce the PL in Yb:IOG10, future studies will include thermal annealing to smoothen the RI-profiles and the investigation of lower numbers of cladding modifications. Recently an investigation of the femtosecond laser induced structural changes in ZBLAN has been published [24]. A similar study with IOG10 can help to compare and understand the differences between both media in the future.

Acknowledgments

The author would like to thank Deutsche Forschungsgemeinschaft for Fellowship funding under GZ: PA1978/1-1. This research was supported by the Australian Research Council Centre of Excellence for Ultrahigh bandwidth Devices for Optical Systems (project number CE110001018) and was performed in part at the OptoFab node of the Australian National Fabrication Facility utilizing Commonwealth and NSW State Government funding.